Cognitive Computation (2019) 11:789–798
https://doi.org/10.1007/s12559-018-9582-9

Clustering of Remote Sensing Imagery Using a Social Recognition-Based Multi-objective Gravitational Search Algorithm

Aizhu Zhang[1,2] · Sihan Liu[3] · Genyun Sun[1,2] · Hui Huang[1,2] · Ping Ma[1,2] · Jun Rong[1,2] · Hongzhang Ma[4] · Chengyan Lin[1,2] · Zhenjie Wang[1,2]

Received: 29 March 2018 / Accepted: 16 July 2018 / Published online: 23 July 2018

Abstract

Cognitively inspired swarm intelligence algorithms (SIAs) have attracted much attention in the research area of clustering since it can give machine the ability of self-learning to achieve better classification results. Recently, the SIA-based multi-objective optimization (MOO) methods have shown their superiorities in data clustering. However, their performances are limited when applying to the clustering of remote sensing imagery (RSI). To construct an excellent MOO-based clustering method, this paper presents a social recognition-based multi-objective gravitational search algorithm (SMGSA) to achieve simultaneous optimization of two conflicting cluster validity indices, i.e., the Xie-Beni (*XB*) index and the J_m index. In the SMGSA, searching particles not only are guided by those elite particles stored in an external archive by the gravitational force but also learn from the social recognition of the whole population through the position difference. SMGSA thereby formed with outstanding exploitation ability. Comparison experiments on two public RSI data sets, including a moderate aerial image and a hyperspectral, validated that the MOO-based clustering methods could obtain more accurate results than the single validity index-based method. Moreover, the SMGSA-based method can achieve superior results than that of the multi-objective gravitational search algorithm without social recognition ability. The proposed SMGSA performs favorable balance between the two conflicting cluster validity indices and achieves preferable classification for the RSI. In addition, this study indicates that the swarm intelligence-based cognitive computing is potential for the intelligent interpretation and understanding of complicated remote sensing scene.

Keywords Social recognition · Swarm intelligence · Multi-objective optimization (MOO) · Gravitational search algorithm (GSA) · Remote sensing image classification

Introduction

Clustering is a kind of unsupervised classification method that partitions a given data set into established groups without any expert knowledge. The traditional clustering method focuses on quantitative and deterministic computing technology from a statistical pattern recognition perspective, but it is not good at solving the imprecise and uncertain problems [1]. In contrast, cognitive computing is a new data-centric computing model which enables self-learning of the computer (algorithms) to achieve improved flexibility to the uncertainty of complex problems [2].

Cognitively inspired swarm intelligence algorithms (SIAs) have attracted wide attention in data clustering and many other scientific and engineering fields [3–6]. In the SIAs, particles usually make decisions according to their own experience or the elite's suggestions. Moreover, the stochastic mechanism is introduced to all the SIAs to promote their optimization capability [7]. Nevertheless, the SIA-based clustering encounters unavoidable difficulty when applied to analysis of the complex remote sensing imagery (RSI).

One crucial issue is the definition of the objective function in the SIA-based clustering method. In most of the previous

✉ Genyun Sun
genyunsun@163.com

1 School of Geosciences, China University of Petroleum (East China), Qingdao 266580, Shandong, China

2 Laboratory for Marine Mineral Resources, Qingdao National Laboratory for Marine Science and Technology, Qingdao 266071, China

3 Satellite Environment Center, Ministry of Environmental Protection of China, Beijing 100094, China

4 College of Science, China University of Petroleum (East China), Qingdao 266580, Shandong, China

researches, the clustering is realized by the iteratively optimization of some validity indices (called objective function in the SIA-based method) [8]. The essence of a clustering validity index is to evolve a partition matrix of the input RSI by optimizing a certain objective function, such as minimization of overall deviation (intra-cluster spread of data), maximization of connectivity (inter-cluster connectivity), minimization of the number of features, or minimization of the error rate of the classifier [9]. That is to say, the objective function to be optimized in the RSI clustering method is a key factor in the whole SIA-based clustering method.

Various validity indices are proposed from different perspectives, which can capture a specific structure of the remote sensing image. Effective clustering can be achieved if there is a good match between the estimated remote sensing image structure and the real one, which is unknown in practice [10]. Hence, there may be no single objective function that can perform well on complex remote sensing images with different structures. Thus, in order to enhance the generalization, SIA-based joint optimization of two or more cluster validity indices has become a new intend to combine their advantages for the effective clustering of RSI [11]. This in essence belongs to the problem of multi-objective optimization (MOO), in which a set of Pareto-optimal solutions is usually produced instead of a single optimal solution [12].

Classical methods for solving MOO problems include the weighted aggregation method and the ε-constraint method. The former usually takes MOO problems as a single-objective optimization (SOO) problem that can be solved using nonlinear optimization methods [13]. The latter commonly selects one objective as the optimized one and trades the others as the constraint conditions of the SOO problem. However, these methods can hardly obtain the whole Pareto-optimal solutions in a single run due to the difficulty in tuning the weights and the constrained parameters [14]. Unlike the traditional mathematical programming methods, the nature-inspired algorithms (NAs) attempt to find multiple Pareto-optimal solutions in a single simulation run [11]. Many NAs, such as particle swarm optimization (PSO) [12], genetic algorithm (GSA) [13–15], artificial bee colony (ABC) [3], evolutionary algorithm (EA) [16], and chemical reaction optimization (CRO) [4], have been extended to solve the MOO problems.

The existing MOO algorithms can be classified into three categories, i.e., the Pareto-based approaches [12, 15, 17], the indicator-based approaches [18, 19], and the decomposition-based method [20, 21]. The Pareto-based approaches, which incorporate the Pareto optimality into the individual update process, are the most popular ones. In this category of MOO algorithms, cooperation of the *Pareto dominance* and diversity maintain operators are crucial for the leader selection and population evolution. For example, in the fast and elitist multi-objective genetic algorithm (NSGA-II) [15], a non-dominated sorting method is proposed to find dominant states of individuals while a crowding distance method is developed for estimating their density while maintaining the diversity of solutions. The non-dominated solutions with a larger crowding distance are more likely to be selected as leaders to direct the cognitive learning of other particles. Recently, some Pareto-based approaches have been successfully applied to the clustering of RSI. Nevertheless, the inherent search ability of the NAs still plays a key role in the optimization of MOO problems, which is also confirmed by the MOO-based RSI clustering [9, 10, 22–26].

The most prominent problem is that many MOO algorithms suffer from premature problems. In [22], two fuzzy clustering validity indices were incorporated into the NSGA-II as the fuzzy clustering methods can be severely affected by the presence of mixed pixels [10]. However, due to the evolutionary algorithm that always overemphasizes on the global search and appears lack of the local search capability, the NSGA-II-based clustering is hard to attain promising solutions and produce the more accurate classification results. Different from the evolutionary algorithm, the memetic algorithm has both the global and local search capabilities. However, when applying to the complex problem, balance between the global search and local search is still a challenging problem in memetic algorithms. Various methods have been attempted to construct the adaptive multi-objective memetic algorithm for better RSI clustering [10, 27].

Gravitational search algorithm (GSA) is a recently proposed swarm intelligence algorithm motivated from Newtonian laws of gravity and motion [28]. In GSA, particles search the optimal solutions following the elites based on social cognitive sciences. Since its presentation, GSA has been found to be a very effective method in solving SOO problems [29–32]. Moreover, GSA has also been adopted for solving MOO problems. For example, Hassanzadeh et al. [33] proposed a multi-objective GSA in which an external archive was used to store the non-dominated solutions as in simple multi-objective PSO. Nobahari et al. [34, 35] presented a non-dominated sorting GSA with the non-dominated sorting concept. Multi-objective GSA also has been analyzed and utilized to the classification of RSI in our previous works [36, 37], where GSA strives for balance between exploration and exploitation by the adaptive adjustment of neighborhood. However, because GSA cannot maintain and utilize the social recognition of the population (*Gb*) in the search process, the basic GSA inclines to confront weak exploitation when handling complex problems [30, 38]. The increasing complexity of the RSIs also desires progressively more effective MOO methods.

Accordingly, in this paper, the direct attraction of *Gb* is incorporated to present a social recognition-based multi-objective GSA (SMGSA) to achieve better clustering of RSIs. Specifically, the velocity and position of each particle in SMGSA are updated based on the global best memory information associated with the *Gb* and the gravitational rules of

basic GSA. Then the SMGSA is introduced to realize simultaneous optimization of two widely used cluster validity measures: the Xie-Beni (*XB*) index [39] and the fuzzy C-means (FCM) (J_m) measure [40].

The remainder of this paper is organized as follows: the"Multi-objective Optimization and Basic GSA" section first briefly describes the formulation of MOO problem and the framework of basic GSA. In the "SMGSA-Based Clustering for Remote Sensing Image" section, details of the proposed SMGSA-based clustering algorithm for RSI are introduced. The experimental setup and results are included in the "Experimental Results and Analysis" section. Finally, the paper is concluded in the "Conclusions" section.

Multi-objective Optimization and Basic GSA

Multi-objective Optimization

Solving a MOO problem requires the simultaneous optimization of a number of different and conflicting objects [41]. The general minimization problem of M objectives can be mathematically stated as:

$$\left.\begin{array}{l}\text{minimize}: f(\boldsymbol{x}) = [f_i(\boldsymbol{x}), \quad i = 1, 2, \ldots, M] \\ \text{subject to the constraints}: g_j(\boldsymbol{x}) \leq 0, \quad j = 1, 2, \ldots, J\end{array}\right\} \quad (1)$$

where $\boldsymbol{x} = [x_1, x_2, \ldots x_D]$, D represents the dimension of the decision variable space. $f_i(\boldsymbol{x})$ is the ith objective function for a MOO problem, and $g_j(\boldsymbol{x})$ is the jth inequality constraint and J is the total number of constraints. The aim of the MOO is to find acceptable x so that $f(x)$ is optimized.

For a given MOO problem, there may exist many acceptable solutions. A few relevant definitions are defined as follows:

Definition 1 (*Pareto dominance*) [42]: A vector $\boldsymbol{u} = [u_1, u_2, \ldots, u_M]$ is said to dominate $\boldsymbol{v} = [v_1, v_2, \ldots, v_M]$ (denoted by $\boldsymbol{u} \succ \boldsymbol{v}$) if and only if $\boldsymbol{u}$ is partially less than $\boldsymbol{v}$, i.e., $\forall_i \in \{1, 2, \ldots, M\}, u_i \leq v_i \wedge \exists\, i \in \{1, 2, \ldots, M\} : u_i < v_i$.

Definition 2 (*Pareto optimality*) [42]: A solution $x \in \Omega$ is said to be Pareto optimal with respect to Ω (Ω is the feasible region, $\Omega \subset S$, where S represents the whole search space) if and only if there is no $x' \in \Omega$ for which $\boldsymbol{v} = f(\boldsymbol{x}') = (f_1(\boldsymbol{x}'), \ldots, f_M(\boldsymbol{x}'))$ dominates $\boldsymbol{u} = f(\boldsymbol{x}') = (f_1(\boldsymbol{x}'), \ldots, f_M(\boldsymbol{x}'))$.

Definition 3 (*Pareto front*) [10]: x is said to be a non-dominated solution, or a Pareto-optimal solution, if $x \in \Omega$ and there are no others that dominate x in Ω. The set of all Pareto-optimal solutions is the Pareto-optimal set (PS), and its mapping in the objective space is the Pareto-optimal front (PF) as shown in Fig. 1.

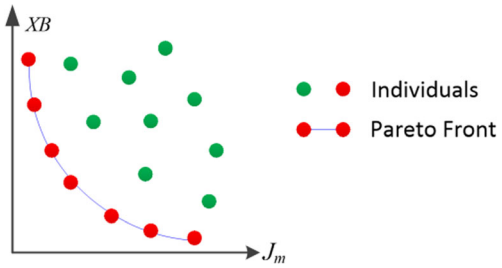

Fig. 1 Illustration of the Pareto front in MOO problem

Fuzzy Clustering

In the fuzzy clustering method, the main objective is to evolve a partition matrix $U(P)$ of the given data set $P = \{P_1, P_2, \ldots, P_N\}$ with K clusters $Z = \{Z_1, \ldots, Z_K\}$. The size of the partition matrix is $K \times N$ and the $U(P)$ can be represented as $U = [u_{kj}]$ where $\sum_{j=1}^{N} u_{kj} \geq 1$, (for $k = 1, 2, \ldots, K$), $\sum_{k=1}^{K} u_{kj} = 1$, ($j = 1, 2, \ldots, N$), $\sum_{k=1}^{K}\sum_{j=1}^{n} u_{kj} = N$.

The J_m measure is the validity measure of fuzzy C-means (FCM). It calculates the global cluster variance, i.e., the within cluster variance summed up over all the clusters as shown in Eq. (2). The J_m needs to be minimized and lower value of J_m indicates better compactness of clusters.

$$J_m = \sum_{k=1}^{N}\sum_{i=1}^{C} u_{ik}^{m} \|\boldsymbol{P}_k - \boldsymbol{z}_i\|^2 \quad (2)$$

where $\boldsymbol{z}_i = \frac{\sum_{k=1}^{N} u_{ik}^{m} \boldsymbol{P}_k}{\sum_{k=1}^{N} u_{ik}^{m}}$ and $u_{ik} = 1/\sum_{j=1}^{C} (\|\boldsymbol{P}_k - \boldsymbol{z}_i\| / \|\boldsymbol{P}_k - \boldsymbol{z}_j\|)^{\frac{2}{m-1}}$, and m is the fuzzy exponent which is set to 2 in this paper.

The *XB* index is defined as a function of the ratio of the total variation to the minimum separation of the clusters. As shown in Eq. (3), *XB* is a combination of global (numerator) and particular (denominator) situations. If the clustering of a RSI is compact and good, the *XB* is shown as a lower value. In other words, the objective of the *XB* index-based clustering is to minimize the value of *XB* for achieving proper clustering.

$$XB = \frac{\sum_{k=1}^{N}\sum_{i=1}^{C} u_{ik}^{m} \|\boldsymbol{P}_k - \boldsymbol{z}_i\|^2}{N \cdot \min\limits_{i \neq j}^{C} \|\boldsymbol{z}_i - \boldsymbol{z}_j\|} \quad (3)$$

where m is the fuzzy exponent which is set to 2 in this paper.

Basic GSA

In the processing of GSA, each particle $\boldsymbol{X}_i = [x_{i1}, x_{i2}, \ldots x_{iD}]$ ($i = \{1, 2, \ldots, NP\}$) is defined as a mass object moves through the D-dimensional search space with a velocity $\boldsymbol{V}_i = [v_{i1}, v_{i2}, \ldots, v_{iD}]$. The velocity of each particle is initialized to zeros and updated relies on the gravitational forces exerted by its neighbors follows the law of gravity [28]. According to the law of gravity, the gravitational force between two particles is

directly proportional to their masses and inversely proportional to their distance. Therefore, we can found that with the gravitational force, the lighter mass will be attracted and moves to the heavier ones. For a population with *NP* particles in GSA, all the particles will move towards those particles that have heavier masses, and ultimately realize the convergence of all particles [28].

Because the mass of particle performs very important role in the processing of GSA, the masses of particles are calculated from their fitness values as follows:

$$nmfit_i^t = \frac{fit_i^t - worst^t}{best^t - \text{worst}^t} \tag{4}$$

$$Mass_i^t = \frac{nmfit_i^t}{\sum_{j=1}^{N} fit_j^t} \tag{5}$$

where t is the current iteration, fit_i^t is the fitness value of the particle i at current time, Mass_i^t represents the mass of particle i, worst_i^t, and best_i^t denotes the worst and best fitness values of a population in the current time. For a maximization problem, worst_i^t and best_i^t are defined by:

$$worst^t = \min_{j\in\{1,2,\ldots,N\}} fit_j^t \tag{6}$$

$$best^t = \min_{j\in\{1,2,\ldots,N\}} fit_j^t \tag{7}$$

For a minimum problem, the definition of worst_i^t and best_i^t is the other way round.

For the gravitational force, the force acting on the particle i from the particle j in each dimension d at the tth iteration is calculated follows:

$$F_{id,jd}^t = G^t \frac{Mass_i^t \times Mass_j^t}{R_{ij}^t + \varepsilon}\left(x_{jd}^t - x_{id}^t\right) \tag{8}$$

where Mass_i^t and Mass_j^t are the masses of the particles i and j in the current iteration; R_{ij}^t is the Euclidian distance between the particles i and j in iteration t; ε is a small positive constant, which is defined as 10^{-6} in this paper; x_{id}^t and x_{jd}^t represent the position of the ith and jth particles in the dth dimension in iteration t; G^t is a decreasing gravitational constant for controlling the search accuracy, which is defined as

$$G^t = G_0 \times \exp\left(-\alpha \times \frac{t}{T_{\max}}\right) \tag{9}$$

where G_0 is the initial value of gravitational constant, α is a decrease coefficient, t is the current iteration, and $T_{\max}$ is the maximum number of iterations. In the basic GSA, the G_0 and α are set to 20 and 100, respectively.

Generally, in the iteration t, the total gravitational force acts on the particle i in the dth dimension, F_{id}^t, should be the sum of all the gravitational forces exerted from other N-1 particles. In the basic GSA, to promote the balance between exploration and exploitation as well as give a stochastic characteristic to GSA, the F_{id}^t is defined as the randomly weighted sum of the forces exerted from K_{best} particles as given below:

$$F_{id}^t = \sum_{j\in K_{best}, j\neq i}^{NP} \text{rand}_j \cdot F_{id,jd}^t \tag{10}$$

where rand_j represents a random number between interval [0, 1], K_{best} is an archive stores the particles ranked in the first K position after fitness sorting in each iteration, and the value of K is initialized as NP in the beginning and linearly decreased with time down to one. Obviously, with the K_{best} model, each particle attracted by less and less particles in the iterations. That is, the exploration fades out while the exploitation fades in as time goes by. Finally, all the particles tend to refine the local area around the global best particle. This operation plays a crucial role in the balance of exploration and exploitation in basic GSA.

Following the obtained gravitational force and the law of motion, the acceleration of the particle i in the dth dimension at iteration t, a_{id}^t, can be obtained by

$$a_{id}^t = \frac{F_{id}^t}{Mass_i^t} \tag{11}$$

Therefore, based on the obtained acceleration, the velocity and the position of the particle i in iteration t can be updated as follows:

$$v_{id}^{t+1} = rand_i \times v_{id}^t + a_{id}^t \tag{12}$$

$$x_{id}^{t+1} = x_{id}^t + v_{id}^{t+1} \tag{13}$$

where rand_i is a uniform random variable in the interval [0, 1].

SMGSA-Based Clustering for Remote Sensing Image

In this paper, a SMGSA-based clustering algorithm for remote sensing image is proposed. In this method, the proposed SMGSA is adapted as the MOO algorithms for simultaneous optimization of the *XB* and J_m indices. The whole process of the multi-objective clustering algorithm is shown in Fig. 2. Accordingly, the SMGSA-based clustering method is a three-step routine: (1) cluster initialization, (2) SMGSA-based cluster updating, and (3) image clustering. The details of each step are given in the following subsections.

Cluster Initialization

In this section, we initialize a population $\boldsymbol{X} = [\boldsymbol{X}_1, \boldsymbol{X}_2, \ldots, \boldsymbol{X}_{N\text{pop}}]$ with N_{pop} particles in a $D\times K$-dimensional search space. Where the D is the bands or size of the feature space

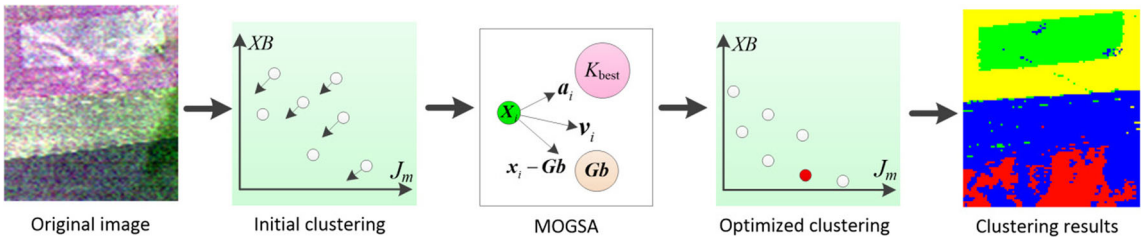

Fig. 2 Flowchart of the SMGSA-based clustering

and K is the number of clusters. That is, each particle $\boldsymbol{X}_i$ denotes a candidate cluster of an input RSI, and the $\boldsymbol{X}_i$ is defined as $\boldsymbol{X}_i = [X_{i1}, X_{i2}, \ldots, X_{iD \times K}]$. The value of each dimension of the particle $\boldsymbol{X}_i$ is randomly generated in the feature space of the RSI. In addition, note that the velocity of each particle is initialized as zeros. An illustration of the cluster initialization is given in Fig. 3.

SMGSA-Based Cluster Updating

After the initialization, SMGSA is applied to update the candidate clusters and search for the Pareto-optimal solutions by minimizing the J_m and XB indices. Flowchart of the SMGSA-based cluster updating operator is shown in Fig. 4 and the details are given in the following steps.

Step 1: Calculation of the objective function

In this paper, the objective function is defined as

$$\min \boldsymbol{f}(\boldsymbol{X}) = [\boldsymbol{f}_1(\boldsymbol{X}), \boldsymbol{f}_2(\boldsymbol{X})] = [J_m, XB] \tag{14}$$

Details of functions J_m and XB are introduced in Eqs. (2) and (3). Therefore, we can obtain two fitness values for each particle.

Step 2: Storage of the non-dominated solutions

Firstly, take comparison the fitness values of the N_{pop} particles and store the position of all the non-dominated solutions to an external archive EXA with a size equals N_{EXA}. Then, we insert all of the currently non-dominated particles into the external archive and remove any dominated particles from the external archive.

Step 3: Generation of hypercubes and assignment of sharing fitness

Following the description in [6], we first generate hypercubes of the search space explored so far, and locate the particles using these hypercubes as a coordinate system where each particle's coordinates are defined according to the values of its objective functions. Then, those hypercubes containing more than one particle are assigned a fitness value equal to the result of dividing any number $num > 1$ (we used $num = 10$ in our experiments) by the number of particles that they contain. This can be seen as a form of fitness sharing. As a result, any hypercube that contains less particles is assigned a smaller fitness values and regarded as with lower density. If external archive reaches the size limitation, particles located in highly populated grids are removed until the size of the external archive satisfies the maximum allowable capacity.

Step 4: Selection of Gb particle

After the assignment of the sharing fitness, we apply roulette-wheel selection using these fitness values to select the hypercube from which we will take the corresponding particle. Therefore, hypercube contains less particle, i.e., with lower density is more likely be selected. Once the hypercube has been selected, we select randomly a particle within such hypercube as the Gb particle.

Step 5: Calculation of acceleration of each particle

In this paper, acceleration of each population particle is attracted by the K_{best} non-dominated solutions stored in EXA. Following Eqs. (9) and (10), we need to calculate the mass of each particle firstly. Because the mass is obtained from the fitness value of particles as shown in Eqs. (4–7), we calculate the mass of each non-dominated solution based on the sharing fitness produced in Eq. (3).

Then, K_{best} non-dominated solutions are selected to exert gravitational force to guide the search behavior of population particles and the acceleration of each population particle can be obtained following Eq. (10). Note that the mass of each population particle is set to unit value and the gravitational

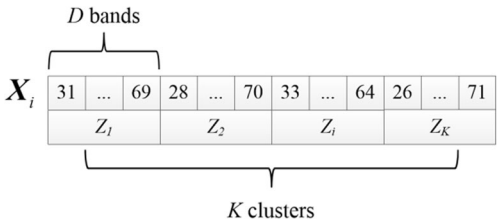

Fig. 3 Example of cluster initialization

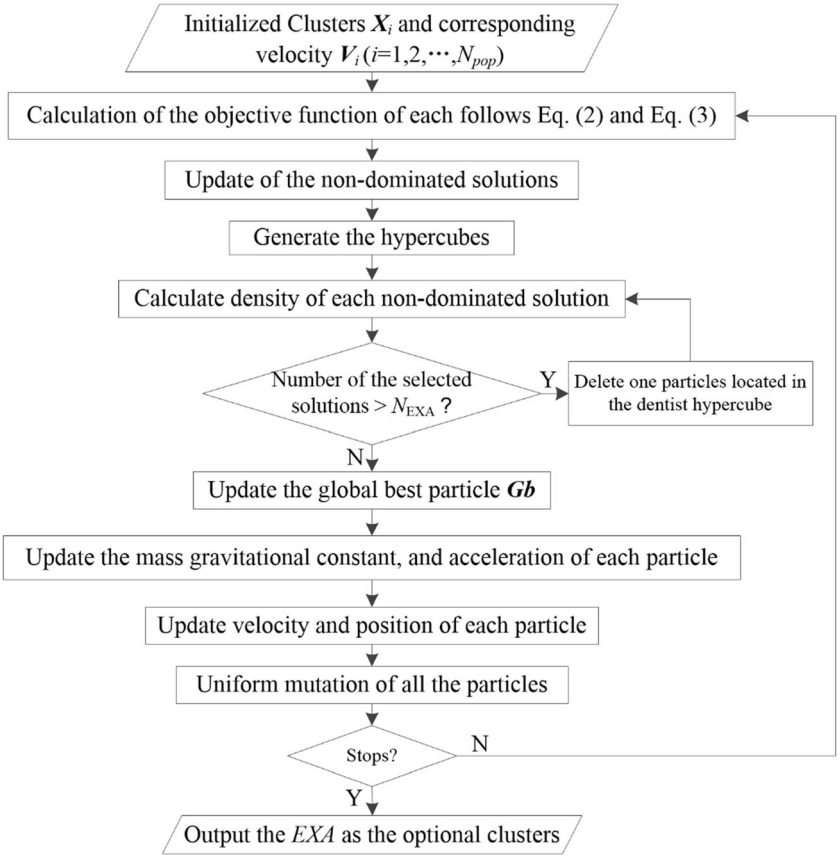

Fig. 4 Flowchart of the SMGSA-based cluster updating operator

constant is calculated following Eq. (11). It is the most important issues in the unembossed problems.

Step 6: Updating of each candidate cluster

In SMGSA, as shown in Eq. (15), each particle updates its velocity by learning from the *Gb* particle according to position difference and the elite particles stored in K_{best} follows acceleration. Then the position of each particle can be updated follows Eq. (16):

$$v_{id}^{t+1} = r_1 \times v_{id}^{t} + r_2 \cdot \left(x_{id}^{t} - Gb_d^{t}\right) + r_3 \cdot a_{id}^{t} \tag{15}$$

$$x_{id}^{t+1} = x_{id}^{t} + v_{id}^{t+1} \tag{16}$$

where r_1, r_2, and r_3 are uniform random variables in the interval [0, 1]. That is, each candidate cluster is updated based on the SMGSA.

Step 7: Usage of mutation operator

GSA has very high convergence speed. However, such convergence speed may be harmful in the context of multi-objective optimization, because a GSA-based algorithm may converge to a false Pareto front (i.e., the equivalent of a local optimum in global optimization). Thereby, a uniform mutation operator is applied to all the population particles to promote the exploration capability of the proposed SMGSA algorithm.

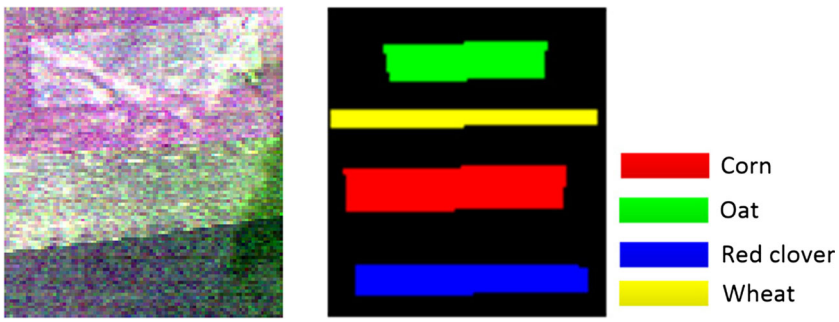

(a) Original image (b) Sample image of FLC image

Fig. 5 FLC image. **a** Original image. **b** Sample image of FLC image

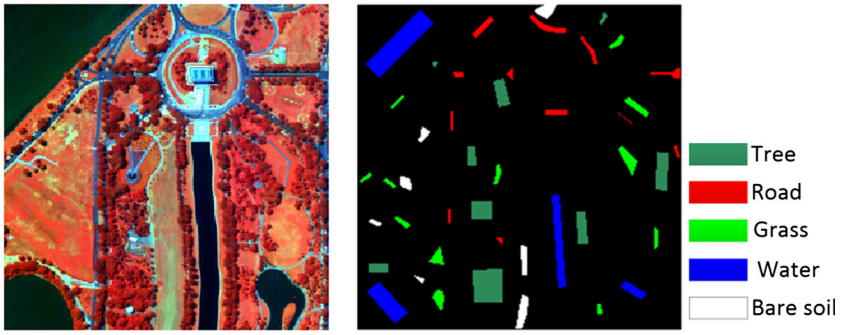

(a) Original image (b) Sampleimage of Washington DC image

Fig. 6 Washington DC image. **a** Original image. **b** Sample image of Washington DC image

Step 8: Stopping criterion

The population X keeps iterative evolution until the stopping criterion reached. In this study, the stopping criterion is the maximum number of fitness evaluations (FEs) which is set to 5000. Finally, a set of non-dominated solutions, i.e., a set of candidate clusters centers are obtained.

Image Clustering

From the above sections, N_{EXA} set of classification results of the tested RSI are produced and users can pick up the most promising one according to their problem requirements. A PMB index [43] is adopted in this paper as a third-party index to select the most appropriate classification result of users. Accordingly, the resultant image clustering results can be outputted.

$$PMB = \left(\frac{1}{K} \times \frac{E_1}{E_K} \times D_K\right)^2, E_k = \sum_{p=1}^{K}\sum_{j=1}^{N_p} \left\|\boldsymbol{x}_j - \boldsymbol{z}_p\right\|, D_K = \max_{i,j=1}^{K} \left\|\boldsymbol{z}_i - \boldsymbol{z}_j\right\| \quad (17)$$

Experimental Results and Analysis

To validate the proposed SMGSA-based clustering algorithm for RSI classification, the original J_m- and XB-based clustering methods, and the NSGSA-based clustering are utilized to perform compared band selection on two public remote sensing images, i.e., the "PLC image" and the "Washington DC image". Both the images can be downloaded from https://engineering.purdue.edu/~biehl/MultiSpec/hyperspectral.html. To perform a fair assessment, for the four algorithms, the population size (N_{pop}) and the external archive size (N_{EXA}) are both set to 100. For J_m and XB, the fuzzy exponent is set to 2. For NSGSA, as suggested in the original paper [35], the reordering and sign mutation probabilities (P_r and P_s) are set to 0.4 and 0.9, respectively. The percent of elitism (P_{elitism}) is set to 0.5; the initial and final values of inertial coefficient (w_0 and w_1) are set to 0.9 and 0.5, respectively. The coefficient of search interval (β) is set to 2.5. For SMGSA, the number of adaptive grid (N_{grid}) is set to 30. The initial gravitational constant and decrease coefficient (G_0 and α) are set to 20 and 100, respectively. All the algorithms were implemented using MATLAB R2017b and executed on a computer with Intel(R) Core™ i3-6100 CPU with 3.70 GHz CPU and 8 GB RAM. In addition, to decrease the influence of randomicity, all the three compared algorithms perform 10 independent runs on each of the data site.

Data Description

FLC Image The FLC image is built by aircraft scanner Flightline C1 in portion of southern Tippecanoe County, Indiana, in 1996. The scanner contains 12 moderate resolution spectral bands. The

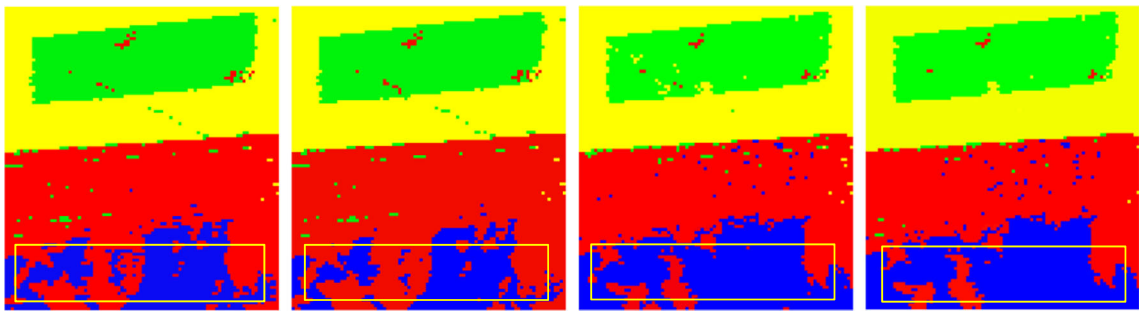

(a) J_m (b) XB (c) NSGSA (d) SMGSA

Fig. 7 FLC image and the clustering results. **a** J_m. **b** XB. **c** NSGSA. **d** SMGSA

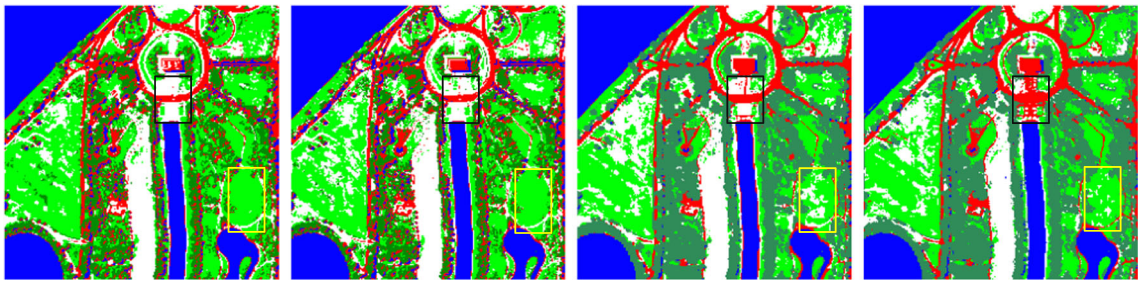

(a) J_m (b) XB (c) NSGSA (d) SMGSA

Fig. 8 Washington DC image and the clustering results. **a** J_m. **b** XB. **c** NSGSA. **d** SMGSA

pseudo-color image with 90 × 100 pixels composed by bands 27 (R), 50 (G), and 127 (B) is shown in Fig. 5a. Figure 5b is a ground reference image that contains four different classes.

Washington DC Image The Washington DC image is acquired by the HYDICE (hyperspectral digital imagery collection experiment) sensor during a flight campaign over Washington DC mall, America. Washington DC image is 250 × 250 pixels with 103 spectral bands. The pseudo-color image composed by bands 79(R), 40 (G), and 4(B) is shown in Fig. 6a. Figure 6b is a ground reference image that contains five different classes.

Experimental Results

Apart from the qualitative comparison of the clustering results produced by the four tested clustering algorithms, we also give the quantitative comparison on the basis of the overall classification accuracy (*OA*) and the kappa coefficient (*kappa*). For the two tested images, the clustering results are presented in Figs. 7 and 8, respectively. The corresponding *OA* and *Kappa* are reported in Table 1.

From Fig. 7, we can see that the clustering results of J_m and *XB* are approximate. Similarly, NSGSA and SMGSA obtained the competitive clustering results. Moreover, the two MOO-based clustering methods show much better results than J_m- and *XB*-based method, especially in the distinguish of red clover and corn (as the yellow rectangle indicated). This may be due to the simultaneous optimization of different indices that makes the clustering algorithm character in the FLC image more accurate. Furthermore, the *OA* and *Kappa* listed in Table 1 also confirm the superiority of NSGSA- and SMGSA-based methods. In addition, from Table 1, we can conclude that although the clustering image of NSGSA and SMGSA are similar, SMGSA in reality performs better clustering than NSGSA in the FLC image.

For the Washington DC image, although the clustering images of NSGSA and SMGSA also looks like each other, as shown in Fig. 8, the MOO-based algorithms exhibits much better clustering results than those of J_m- and *XB*-based methods. Especially, in the identification of the trees (bottle-green in Fig. 8), the MOO-based algorithms show much better capability. Moreover, the confusion of water and road, as well as the confusion of grass and bare soil (as the yellow rectangle indicated) in the results of MOO-based algorithms are much less than that of the single validity-based algorithms as shown in Fig. 8. Furthermore, the SMGSA-based method has the best identification performance for the road, especially for the highlighting road as indicated by the black rectangles in Fig. 8. This may come from the cooperation of the *Gb* particles and the other non-dominated particles that have enhance the exploitation ability of NMPGSA. In addition, the quantitative comparison results listed in Table 1 also shows that the MOO-based clustering methods can produce better classification results than that of the single validity index-based method, and the SMGSA-based method can yield more accurate classification than the SMGSA.

Table 1 Classification results of the two tested images

Images	Methods	*OA* (%)	Kappa
FLC image	J_m	86.64	84.21
	XB	87.53	83.80
	NSGSA	89.75	91.83
	SMGSA	*90.22*	*92.44*
Washington DC image	J_m	89.33	85.54
	XB	89.72	85.15
	NSGSA	92.34	89.09
	SMGSA	*93.26*	*90.47*

Note that the best result in each column is in italics

Conclusions

Traditional clustering method is focusing on deterministic computing technology from a statistical pattern recognition perspective, but it is not good at solving the clustering of remote sensing imagery which has serious uncertainty caused by the mixed pixels. The cognitive computing, especially the cognitively inspired swarm intelligence algorithms, can give machine the ability of self-learning to achieve better flexibility to the uncertainty of complex problems.

This paper presented a novel cognitively inspired algorithm, namely the social recognition-based multi-objective gravitational search algorithm (SMGSA), for the optimal clustering of remote sensing imagery. In SMGSA, each particles search for the non-dominated solutions by learning from two kinds of leaders: (1) the elite particles stored in the K_{best} and (2) the social recognition, i.e., the global best memory of the population. The former exerted guidance to a particle by the gravitational forces while the latter attracted the particle directly. Cooperation of these two kinds of leaders effectively promotes the search ability of SMGSA. Especially the *Gb* particle makes the algorithm pay more attention to the refined recognition and exploitation around the promising areas. When extending SMGSA for image clustering, the SMGSA is utilized to simultaneously optimize the *XB* index and the J_m index. Optimization of the two validity indices can capture the data characteristics of remote sensing imagery better than the single validity index, and thereby achieve better clustering results.

We conducted experiments with two remote sensing imageries to validate the effectiveness of the proposed method. The obtained results are compared with those of the *XB*, J_m, and NSGSA. The comparison results confirmed that the multi-objective-based clustering methods could produce better classification results than that of the single validity index-based method. Moreover, the SMGSA-based method can yield more accurate classification than the NSGSA. Note that because the utilized objective functions are all unsupervised clustering indices, neither the expert knowledge nor the spatial information has been used in the proposed method. Therefore, the clustering results have many finely spots. In the future work, we will focus on the construction of more effective objective functions for more accurate classification of RSI.

Funding This study was funded by the National Natural Science Foundation of China (41471353), the Natural Science Foundation of Shandong Province (ZR201709180096, ZR201702100118), the Fundamental Research Funds for the Central Universities (18CX05030A, 18CX02179A), and the Postdoctoral Application and Research Projects of Qingdao (BY20170204).

Compliance with Ethical Standards

Conflict of Interest The authors declare that they have no conflict of interest.

Ethical Approval This article does not contain any studies with human participants or animals performed by any of the authors.

References

1. Huang XX, Huang HX, Liao BS, et al. An ontology-based approach to metaphor cognitive computation. Mind Mach. 2013;23(1):105–21.
2. Ding S, Zhang J, Jia H, et al. An adaptive density data stream clustering algorithm. Cogn Comput. 2016;8(1):30–8.
3. Kim SS, McLoone S, Byeon JH, et al. Cognitively inspired artificial bee colony clustering for cognitive wireless sensor networks. Cogn Comput. 2017;9(2):207–24.
4. Siddique N, Adeli H. Nature-inspired chemical reaction optimisation algorithms. Cogn Comput. 2017;9(4):411–22.
5. Nanda SJ, Panda G. A survey on nature inspired metaheuristic algorithms for partitional clustering. Swarm Evol Comput. 2014;16:1–18.
6. Chakraborty S, Dey N, Samanta S, et al. Optimization of non-rigid demons registration using cuckoo search algorithm. Cogn Comput. 2017;9(6):817–26.
7. Tang Q, Shen Y, Hu C, et al. Swarm intelligence: based cooperation optimization of multi-modal functions. Cogn Comput. 2013;5(1):48–55.
8. Mukhopadhyay A, Bandyopadhyay S, Maulik U. Clustering using multi-objective genetic algorithm and its application to image segmentation[C]//Systems, Man and Cybernetics, 2006. SMC'06 IEEE International Conference on IEEE. 2006;3:2678–2683.
9. Bong CW, Rajeswari M. Multi-objective nature-inspired clustering and classification techniques for image segmentation. Appl Soft Comput. 2011;11:3271–82.
10. Ma A, Zhong Y, Zhang L. Adaptive multiobjective memetic fuzzy clustering algorithm for remote sensing imagery. IEEE Trans Geosci Remote Sens. 2015;53(8):4202–17.
11. Srinivas N, Deb K. Muiltiobjective optimization using nondominated sorting in genetic algorithms. Evol Comput. 1994;2(3):221–48.
12. Coello CAC, Pulido GT, Lechuga MS. Handling multiple objectives with particle swarm optimization. IEEE Trans Evol Comput. 2004;8:256–79.
13. Mousa AA, El-Shorbagy MA, Abd-El-Wahed WF. Local search based hybrid particle swarm optimization algorithm for multiobjective optimization. Swarm Evol Comput. 2012;3:1–14.
14. Miettinen, K. Nonlinear multiobjective optimization, Springer Science & Business Media; 2012.
15. Deb K, Pratap A, Agarwal S, et al. A fast and elitist multiobjective genetic algorithm: NSGA-II. IEEE Trans Evol Comput. 2002;6(2):182–97.
16. Zitzler E, Deb K, Thiele L. Comparison of multiobjective evolutionary algorithms: empirical results. Evol Comput. 2014;8(2):173–95.
17. Zitzler E, Laumanns M, Thiele L. SPEA2: improving the strength Pareto evolutionary algorithm. In: Giannakoglou K, Tsahalis DT, Périaux J, Papailiou KD, Fogarty T, editors. Evolutionary methods for design, optimization and control with applications to industrial problems. Berlin: Springer-Verlag; 2002. p. 95–100.
18. Zitzler E, Künzli S. Indicator-based selection in multiobjective search[C]//International Conference on Parallel Problem Solving from Nature. Springer, Berlin, Heidelberg; 2004:832–842.
19. Phan DH, Suzuki J. R2-IBEA: R2 indicator based evolutionary algorithm for multiobjective optimization[C]//Evolutionary Computation (CEC), 2013 IEEE Congress on. IEEE; 2013:1836–1845.
20. Zhang Q, Li H. MOEA/D: a multiobjective evolutionary algorithm based on decomposition[J]. IEEE Trans Evol Comput. 2007;11(6):712–31.
21. Liu H L, Gu F, Cheung Y. T-MOEA/D: MOEA/D with objective transform in multi-objective problems[C]//Information Science and Management Engineering (ISME), 2010 International Conference of. IEEE; 2010;2:282–285.
22. Bandyopadhyay S, Maulik U, Mukhopadhyay A. Multiobjective genetic clustering for pixel classification in remote sensing imagery. IEEE Trans Geosci Remote Sens. 2007;45:1506–11.
23. Mukhopadhyay A, Maulik U. Unsupervised pixel classification in satellite imagery using multiobjective fuzzy clustering combined

with SVM classifier. IEEE Trans Geosci Remote Sens. 2009;47(4):1132–8.
24. Paoli A, Melgani F, Pasolli E. Clustering of hyperspectral images based on multiobjective particle swarm optimization. IEEE Trans Geosci Remote Sens. 2009;47(12):4175–88.
25. Zhang M, Jiao L, Ma W, et al. Multi-objective evolutionary fuzzy clustering for image segmentation with MOEA/D. Appl Soft Comput. 2016;48:621–37.
26. Zhong Y, Zhang S, Zhang L. Automatic fuzzy clustering based on adaptive multi-objective differential evolution for remote sensing imagery. IEEE J-STARS. 2013;6(5):2290–301.
27. Zhong Y, Ma A, Zhang L. An adaptive memetic fuzzy clustering algorithm with spatial information for remote sensing imagery. IEEE J-STARS. 2014;7(4):1235–48.
28. Rashedi E, Nezamabadi-Pour H, Saryazdi S. GSA: a gravitational search algorithm. Inform Sciences. 2009;179(13):2232–48.
29. Han X, Chang X, Quan L, et al. Feature subset selection by gravitational search algorithm optimization. Inf Sci. 2014;281:128–46.
30. Mirjalili S, Lewis A. Adaptive gbest-guided gravitational search algorithm. Neural Comput & Applic. 2014;25(7–8):1569–84.
31. Zhang A, Sun G, Wang Z, et al. A hybrid genetic algorithm and gravitational search algorithm for global optimization. Neural Netw World. 2015;25(1):53–73.
32. Zhang A, Sun G, Ren J, et al. A dynamic neighborhood learning-based gravitational search algorithm. IEEE Transactions on Cybernetics. 2018;48(1):436–47.
33. Hassanzadeh H R, Rouhani M. A multi-objective gravitational search algorithm[C]//Computational Intelligence, Communication Systems and Networks (CICSyN), 2010 Second International Conference on. IEEE Int Conf Comput Intell Commun Syst (CICSyN); 2010:7–12.
34. Nobahari H, Nikusokhan M, Siarry P. Non-dominated sorting gravitational search algorithm[C]//Proc. of the 2011 International Conference on Swarm Intelligence, ICSI; 2011:1–10.
35. Nobahari H, Nikusokhan M, Siarry P. A multi-objective gravitational search algorithm based on non-dominated sorting[J]. International Journal of Swarm Intelligence Research (IJSIR). 2012;3(3):32–49.
36. Sun G, Zhang A, Jia X, et al. DMMOGSA: diversity-enhanced and memory-based multi-objective gravitational search algorithm. Inform Sciences. 2016;363:52–71.
37. Zhang A, Sun G, Wang Z. Remote sensing imagery classification using multi-objective gravitational search algorithm[C]//Image and Signal Processing for Remote Sensing XXII. International Society for Optics and Photonics. 2016;10004:100041I.
38. Yin B, Guo Z, Liang Z, et al. Improved gravitational search algorithm with crossover. Comput Electr Eng. 2017.
39. Xie XL, Beni G. A validity measure for fuzzy clustering. IEEE Trans Pattern Anal Mach Intell. 1991;13(8):841–7.
40. Bezdek JC. Pattern recognition with fuzzy objective function algorithms. USA: Plenum Press; 1981.
41. Guo W, Wang L, Wu Q. Numerical comparisons of migration models for multi-objective biogeography-based optimization. Inf Sci. 2016;328:302–20.
42. Mirjalili S, Saremi S, Mirjalili SM, et al. Multi-objective grey wolf optimizer: a novel algorithm for multi-criterion optimization. Expert Syst Appl. 2016;47:106–19.
43. Maulik U, Bandyopadhyay S. Performance evaluation of some clustering algorithms and validity indices. IEEE Trans Pattern Anal Mach Intell. 2002;24(12):1650–4.